Journal of The Electrochemical Society, **154** (7) B694-B699 (2007)
0013-4651/2007/154(7)/B694/6/$20.00 © The Electrochemical Society

An Examination of SOFC Anode Functional Layers Based on Ceria in YSZ

M. D. Gross, J. M. Vohs,* and R. J. Gorte*,z

Department of Chemical and Biomolecular Engineering, University of Pennsylvania, Philadelphia, Pennsylvania 19104, USA

The properties of solid oxide fuel cell (SOFC) anode functional layers prepared by impregnation of ceria and catalytic metals into porous yttria-stabilized zirconia (YSZ) have been examined for operation at 973 K. By varying the thickness of the functional layer, the conductivity of the ceria-YSZ composite was determined to be only 0.015–0.02 S/cm. The initial performance of anodes made with ceria loadings of 40 or 60 wt % were similar but the anodes with lower loadings lost conductivity above 1073 K due to sintering of the ceria. The addition of dopant levels of catalytic metals was found to be critical. The addition of 1 wt % Pd or Ni decreased the anode impedances in humidified H_2 dramatically, while the improvement with 5 wt % Cu was significant but more modest. Pd doping also decreased the anode impedance in dry CH_4 much more than did Cu doping; however, addition of either Pd or Cu led to similar improvements for operation in *n*-butane. Based on these results, suggestions are made for ways to improve SOFC anode functional layers.
 [DOI: 10.1149/1.2736647]

Manuscript submitted January 4, 2007; revised manuscript received March 8, 2007. Available electronically May 22, 2007.

While the large majority of solid oxide fuel cells (SOFCs) have anodes made from ceramic-metallic (cermet) composites of Ni with yttria-stabilized zirconia (YSZ),[1,2] there has recently been significant interest in developing alternative anodes to avoid some of the important limitations of Ni-based electrodes. In particular, Ni composites are sensitive to sulfur,[3] can form carbon deposits in the presence of hydrocarbon fuels,[4] and are intolerant of oxidation cycles.[5] Anodes based on conductive ceramics are especially attractive for replacing Ni cermets because it is anticipated that they should be insensitive to redox cycling and could exhibit high thermal stability.[6-12] Furthermore, at least some conductive ceramics have demonstrated tolerance to sulfur[12] and resistance to carbon formation in the presence of hydrocarbons.[6] In most cases, however, ceramic anodes have also led to much higher overpotentials than are commonly achieved with Ni–YSZ cermets. The modest electrochemical performance of ceramic anodes is due to the difficulty of producing ceramics that have both high electronic and ionic conductivity at low $P(O_2)$, while also having good surface reactivity with H_2 and other fuels.[6]

We have recently reported that it is possible to obtain good ceramic anode performance, without having to develop new oxide compositions, through the use of separate functional and conduction layers.[13] That study demonstrated that low anode overpotentials could be achieved if the materials used in the functional layer had sufficient catalytic activity, even if those materials had only modest electronic conductivity. Ohmic losses associated with poor electronic conductivity in the functional layer were kept low by making the functional layers very thin, on the order of 10 μm. Current collection was accomplished primarily within a thicker conduction layer in which electrochemical activity was unnecessary, so that similar performance was achieved when using either Ag paste or porous $La_{0.3}Sr_{0.7}TiO_3$ (LST) for electronic conduction. The functional layer in the previous study was made from 1 wt % Pd and 40 wt % ceria, impregnated into 65% porous YSZ. Pd-doped ceria was chosen in that study because ceria provides some electronic conductivity under reducing conditions and Pd/ceria is one of the most active catalysts known for hydrocarbon oxidation.[14]

In the present research, we examined the role of the functional layer in more detail. While we continued to prepare the functional layer by impregnation methods, we examined the role of functional layer thickness and composition more carefully, particularly looking toward avoiding the use of precious metals and application of ceramic anodes with other fuels. The results further demonstrate the promise of using the functional layer approach for developing ceramic anodes and point toward directions for further improvements.

Experimental

The first step in preparing the fuel cells used here involved making a YSZ wafer that had a dense layer between two porous layers. Both anodes and cathodes were then fabricated by impregnation of the active components into the porous layers. The porous-dense-porous YSZ structure was produced by laminating three green tapes, using pore formers in the layers that were to be porous, and then firing the structure to 1823 K for 4 h.[15] The green tapes were prepared by mixing YSZ powder (Tosoh Corp., 8 mol % Y_2O_3-doped ZrO_2, 0.2 μm) with distilled water, a dispersant (1.27 g, Duramax 3005, Rohm & Haas), and binders (10.2 g HA12 and 14.4 g B1000, Rohm & Haas). On each of the cells, the dense electrolyte layer was 50 μm thick and the porous YSZ used in the cathode layer was 300 μm thick. The cathode layer was infiltrated with aqueous solutions of $La(NO_3)_3{\cdot}6H_2O$, $Sr(NO_3)_2$, and $Fe(NO_3)_3{\cdot}9H_2O$ to produce a composite of YSZ with $La_{0.8}Sr_{0.2}FeO_3$ (LSF), as described elsewhere.[16] For the present investigation, it is only important to recognize that the LSF-YSZ has a current-independent impedance of 0.1 to 0.15 Ω cm^2 at 973 K.[16]

The thickness of the 65% porous YSZ used in making the functional layer of the anodes was either 12, 50, or 100 μm, and the porosity was introduced through the addition of graphite (GE, Alfa Aeser, 325 mesh, conductivity grade) into the green tape. Ceria was added to this layer by impregnation of an aqueous solution of $Ce(NO_3)_3{\cdot}6H_2O$, followed by calcination at 723 K. After addition of ceria, a catalytic metal was added by impregnation of either $(NH_3)_4Pd(NO_3)_2$, $Ni(NO_3)_2{\cdot}6H_2O$, or $Cu(NO_3)_2{\cdot}6H_2O$, followed by calcination at 723 K in air. The conduction layer was simply Ag paste applied to the surface of the electrode, and Ag was also applied for current collection at the cathode.

For testing, the cells were attached to an alumina tube with a ceramic adhesive (Aremco, Ceramabond 552). The external area of each fuel electrode was 0.33 cm^2 but the areas of the electrolyte and cathode were ~1 cm^2. All of the performance calculations assumed an active area of 0.33 cm^2, which may underestimate the active cathode area by as much as 9%,[17] but should properly reflect the area-specific performance of the anode. Impedance spectra were measured in the galvanostatic mode with a frequency range of 0.1 Hz to 100 kHz and a 1 mA ac perturbation with a Gamry Instruments potentiostat. Humidified H_2 (3% H_2O) was introduced into the anode compartment by first passing the H_2 through a room-temperature bubbler.

* Electrochemical Society Active Member.
z E-mail: gorte@seas.upenn.edu

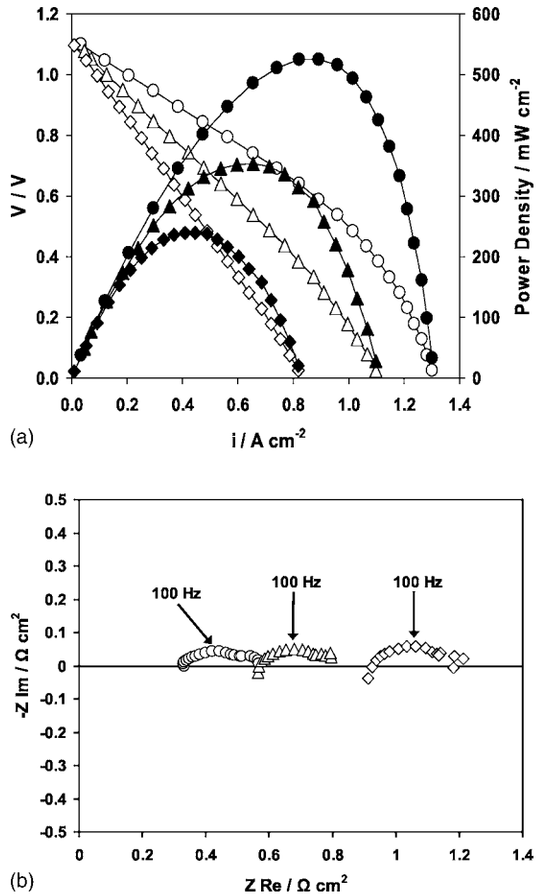

Figure 1. (a) V-i polarization curves and (b) impedance spectra for Ce–Pd–YSZ anodes with 40 wt % CeO_2 and 1 wt % Pd in humidified H_2 (3% H_2O) at 973 K. Data is shown for the following anode thicknesses: circles, 12 μm, triangles, 50 μm, and diamonds, 100 μm.

Results

Anode thickness.— To test our earlier hypothesis that an anode functional layer need have only minimal electronic conductivity if it has sufficient catalytic activity, we reexamined the effect of varying the thickness of the functional layer in cells prepared with 40 wt % ceria and 1 wt % Pd. Cells were prepared that were identical except for having anode thicknesses of 12, 50, and 100 μm. In each case, the electrolyte thickness was 50 μm and the cathode was an LSF-YSZ composite prepared by impregnation methods. Figure 1 shows V-i polarization curves and open-circuit impedance results for these cells at 973 K in humidified H_2. Figure 1a shows that the performance of the cells decreased in a regular manner as the thickness of the anode functional layer increased, going from a maximum power density of 520 mW/cm^2 for the 12 μm anode to approximately 230 mW/cm^2 for the 100 μm anode. The Cole-Cole plots in Fig. 1b demonstrate that the loss in performance is almost entirely caused by an increase in ohmic resistance in the cells with thicker functional layers. Each cell exhibited a nonohmic impedance of $\sim$0.3 Ω cm^2, while the ohmic resistance increased from 0.33 Ω cm^2 for the 12 μm anode to 0.93 Ω cm^2 for the 100 μm anode. These ohmic resistances are listed in Table I.

Using a literature value for the conductivity of YSZ at 973 K,[18] the contribution to the ohmic resistance from a 50 μm electrolyte was calculated to be 0.27 Ω cm^2, implying that the remaining ohmic losses were due to poor conductivity within the functional layer of the anode. The cathode used in this study is expected to have negligible ohmic resistance.[16] In Table I, we have subtracted the electrolyte contribution to the ohmic resistance and calculated the conductivities of the functional layers from the excess ohmic resistance and the functional layer thickness. Independent of functional layer thickness, the conductivity values ranged from 0.020 to 0.015 S/cm, values that are in good agreement with the conductivity reported from four-probe measurements of ceria impregnated into porous YSZ.[19] The agreement with previous four-probe measurements also shows that conductivity in these anodes cannot be due to penetration of the Ag ink into the porous YSZ.

Table I. Total ohmic resistance, anode contribution to the ohmic resistance, and calculated conductivity of CeO_2–Pd–YSZ anodes with 40 wt % CeO_2 and 1 wt % Pd at 973 K in humidified (3%H_2O) H_2 for various anode thicknesses.

Thickness	$R_{\Omega\ \text{total}}$ (Ω cm^2)	$R_{\Omega\ \text{anode}}$ (Ω cm^2)	σ_{anode} (S cm^{-1})
12 μm	0.33	0.06	0.020
50 μm	0.57	0.30	0.017
100 μm	0.93	0.66	0.015

The ohmic losses within the functional layers remain higher than is desirable, even for the 12 μm anode. Note, however, that the nonohmic contribution to the electrode impedance is essentially independent of functional layer thickness and that reasonable anode performance can be achieved with a material that has such poor conductivity. This is important in proving that materials with modest conductivity could provide good performance.

The effect of ceria loading.— The simplest way to modify the anode functional layer performance is through changing the ceria loading. To test the effect of this parameter, cells with 12 μm layers of porous YSZ were impregnated with 1 wt % Pd and 20, 40, or 60 wt % ceria. The V-i polarization curves and Cole-Cole plots of the open-circuit impedance data at 973 K in humidified H_2 are shown in Fig. 2 for each of these cells. Figure 2a demonstrates that performance of the cell with only 20 wt % ceria is notably worse than the cells with higher ceria loadings, showing a maximum power density of only 360 mW/cm^2. The cells with 40 and 60 wt % ceria both had power densities approaching 520 mW/cm^2. The reason for the lower performance with 20 wt % ceria is clear from the impedance data in Fig. 2b. The ohmic resistance of the cell with only 20 wt % ceria was 0.45 Ω cm^2. The nonohmic impedance of the cell with 20 wt % ceria was also larger but this may be related to the increased ohmic contribution.[19] Given that 20 wt % ceria corresponds to less than 10 vol % of the anode functional layer, a value well below the 30 vol % required to achieve the percolation threshold required for random media, it is not surprising that this loading is insufficient.

While the initial results for the cells with 40 and 60 wt % ceria were nearly identical, the stability of the cell with 60 wt % ceria was significantly better. This was observed from measurements of the ohmic resistance of all three cells at 973 K in humidified H_2, before and after heating the cells to 1073 K for 2 h. The results reported in Table II show that the ohmic resistances increased for all of the cells but that the cell with 60 wt % ceria showed the smallest increase, going from 0.32 to 0.34 Ω cm^2. To determine whether even higher temperatures would increase the deterioration of the cell performance, the cell with 60 wt % ceria was heated to 1173 K for an additional 80 h before again testing it at 973 K. The additional treatment increased the ohmic resistance to 0.44 Ω cm^2.

It is likely that this loss of conductivity results from sintering of the ceria that coats the YSZ pores, either due to decreased connectivity in the ceria layer or a lower surface conductivity of high-temperature ceria. Previous studies have reported that ceria films on YSZ have considerable mobility at temperatures similar to that used here,[20] and that this mobility is a strong function of the gas-phase environment.[21] To determine whether or not the increase in ohmic resistance could be attributed to a loss of conductivity in the ceria-

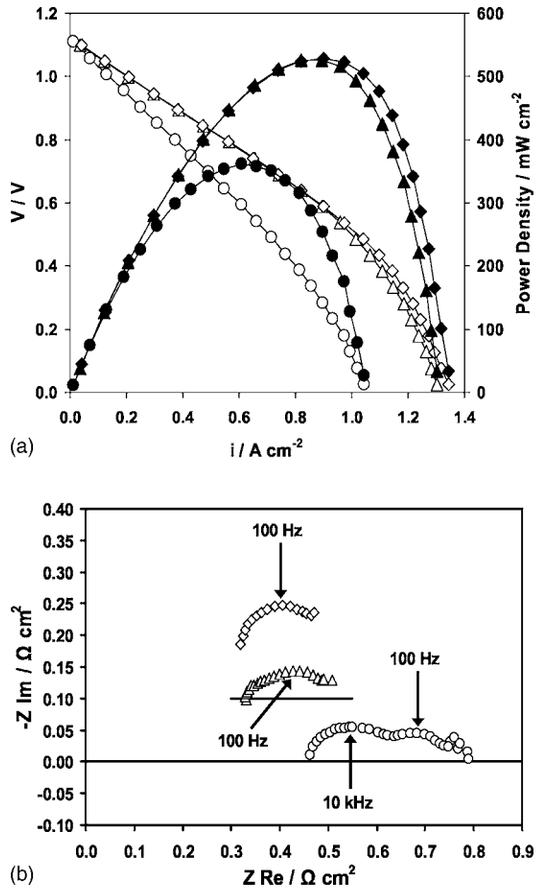

Figure 2. (a) V-i polarization curves and (b) impedance spectra for 12 μm Ce–Pd–YSZ anodes with 1 wt % Pd in humidified H_2 (3% H_2O) at 973 K. Data is shown for the following CeO_2 loadings: circles, 20 wt %, triangles, 40 wt %, and diamonds, 60 wt %.

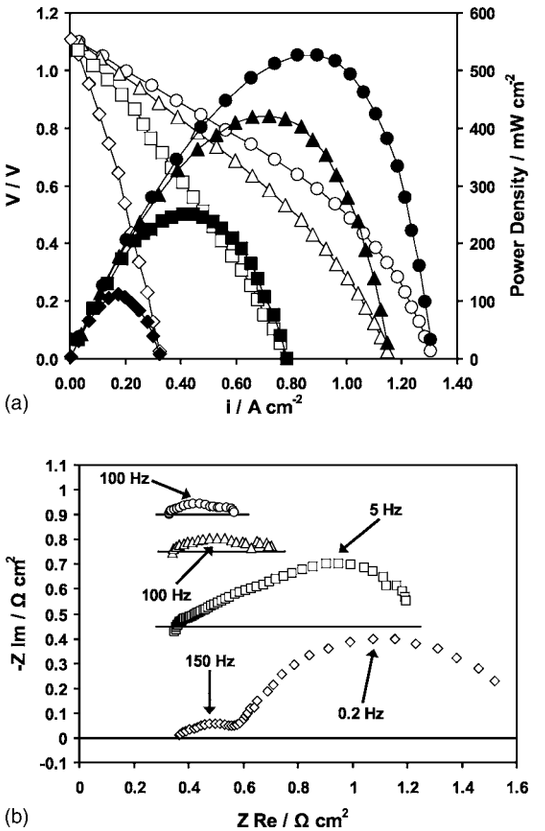

Figure 3. (a) V-i polarization curves and (b) impedance spectra for 12 μm CeO_2–M–YSZ anodes with 40 wt % CeO_2 in humidified H_2 (3% H_2O) at 973 K. Data is shown for the following metal (M) dopants: circles, 1 wt % Pd, triangles, 1 wt % Ni, squares, 5 wt % Cu, and diamonds, no metal.

YSZ layer, conductivity tests were performed on a YSZ slab, 1 × 1 × 10 mm, impregnated with 40 wt % ceria and 1 wt % Pd, using the standard four-probe method. The slab was made from the same slurry used in making the tapes for the function layers. The conductivity of the slab at 973 K in humidified H_2 decreased from 0.020 to 0.018 S/cm after heating to 1073 K for 2 h. After heating to 1173 K in humidified H_2 for 20 h, the conductivity further decreased to 0.013 S/cm. These results support the idea that the increased ohmic resistance of the cells following high-temperature treatment is due to loss of conductivity of the functional layer. Clearly, the conductivity of the functional layers prepared by impregnation of ceria needs to be stabilized for high-temperature treatment.

Table II. Ohmic resistance of 12 μm CeO_2–Pd–YSZ anodes with 1 wt % Pd and variable CeO_2 loadings measured in humidified H_2 (3%H_2O) at 973 K after the following heat-treatments: 973 K for 2 h, 1073 K for 2 h, and 1173 K for 80 h.

CeO_2 loading	973 K R_Ω (Ω cm^2)	973 K after 1073 K 2 h R_Ω (Ω cm^2)	973 K after 1173 K 80 h R_Ω (Ω cm^2)
20 wt % CeO_2	0.46	0.57	
40 wt % CeO_2	0.33	0.38	
60 wt % CeO_2	0.32	0.34	0.44

Comparison of Pd, Ni, and Cu Catalysts.— All of the above measurements used anode functional layers with 1 wt % Pd because our earlier study showed that a catalytic metal was essential for good anode performance.[13] While the amounts of Pd that were added to the functional layer were small, it would obviously be better if good performance could be achieved using base-metal catalysts, without the addition of precious metals.

Therefore, we compared the performance of electrodes made by impregnating 65% porous YSZ with 40 wt % CeO_2, to which an additional 1 wt % Pd, 1 wt % Ni, or 5 wt % Cu was added for catalytic purposes. The anode functional layer was 12 μm thick in each case. Ni was chosen for comparison to Pd because it exhibits comparable catalytic activity for oxidation reactions under conditions where it remains reduced. While Cu-ceria catalysts are active for the water-gas-shift reaction and for reforming of alcohols,[22-24] Cu is a relatively poor oxidation catalyst. We therefore chose to use a higher loading for Cu relative to the other metals. In each case, the metal loadings were significantly below the percolation threshold for electronic conduction and electronic conductivity within the functional layers was provided solely by the doped-CeO_2.

Figure 3a shows V-i polarization curves at 973 K in humidified H_2 for four identical fuel cells made with each of the three metal catalysts and without the addition of any metal. The corresponding impedance spectra, measured at open-circuit, are reported in Fig. 3b. The maximum power density of the cell with the ceria-only anode was 110 mW/cm^2 and the impedance data demonstrates that most of the cell losses are associated with electrode polarization. The cell performance improved dramatically upon the addition of Pd or Ni, to maximum power densities of 520 and 420 mW/cm^2, respectively. Essentially all of the improvement is associated with a decrease in

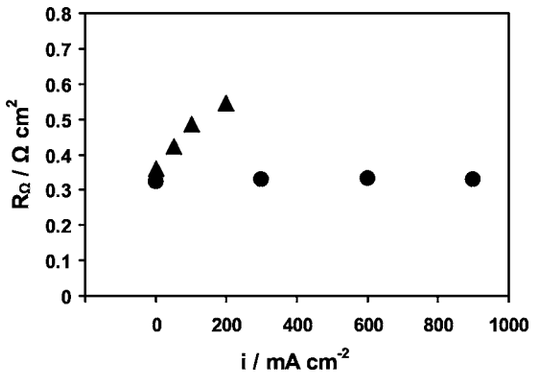

Figure 4. Ohmic resistance as a function of current density for 12 μm CeO_2–M–YSZ anodes with 40 wt % CeO_2 in humidified H_2 (3% H_2O) at 973 K. Data is shown for the following metal (M) dopants: circles, 1 wt % Pd, and diamonds, no metal.

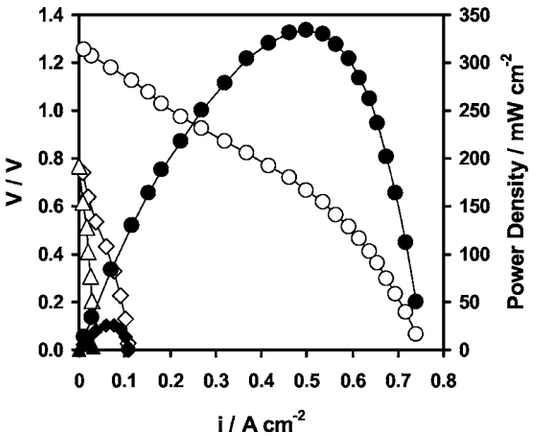

Figure 5. (a) V-i polarization curves for 12 μm CeO_2–M–YSZ anodes with 40 wt % CeO_2 in dry CH_4 at 973 K. Data is shown for the following metal (M) dopants: circles, 1 wt % Pd, diamonds, 5 wt % Cu, and triangles, no metal.

the electrode impedances, from more than 1.2 Ω cm^2 when no metal was added, to 0.25 Ω cm^2 upon the addition of Pd and 0.35 Ω cm^2 upon the addition of Ni. Because the LSF-YSZ cathode is expected to have an electrode impedance of 0.1 Ω cm^2 at 973 K, the nonohmic losses for the Pd and Ni containing cells were between 0.15 and 0.25 Ω cm^2. While there was a slight decrease in the ohmic resistance upon the addition of the catalytic metals, the primary change that occurred upon the addition of Pd or Ni was the loss of a large arc at 0.2 Hz in the Cole-Cole plots.

The cell containing 5 wt % Cu exhibited lower performance than the cells with Pd or Ni, but its performance was significantly better than the cell without added metal. The maximum power density improved to 250 mW/cm^2 upon the addition of Cu and the total nonohmic impedance decreased to approximately 0.9 Ω cm^2. It is most interesting that performance characteristics of the Cu-containing cell are reasonably close to those reported in earlier studies of cells with Cu-ceria-YSZ anodes and LSF-YSZ cathodes,[16] which used thicker anodes and sufficient amounts of Cu to make the electrode conductive. This similarity leads to two conclusions. First, Cu, in combination with ceria, is capable of providing some electrochemical activity to the anode. This contradicts an earlier conclusion from our laboratory, based on the fact that similar performance levels were achieved using Au-ceria and Cu-ceria anodes.[25] The ability to separate electronic conductivity from catalytic activity through the use of thin anode functional layers makes the present study more sensitive to the relatively low enhancement that Cu provides. Second, the similarity in the performance of cells with 12 μm Cu-ceria functional layers to that of cells with thick Cu-ceria electrodes suggests that all of the electrochemical activity occurs within approximately 10 μm of the electrolyte in both cases.

The impedance data at open circuit in Fig. 3b indicate that the ohmic resistances in all four cells were 0.34 ± 0.02 Ω cm^2. With 0.26 Ω cm^2 of this coming from the 50 μm electrolyte, the ohmic losses associated with each of the anode functional layers must be approximately 0.08 Ω cm^2. While there was no significant difference in the ohmic resistance of cells that contained catalytic metals and the one that did not at open circuit, we observed a significant increase in the ohmic resistance of the cell that had no catalytic metal upon application of current. This is shown in Fig. 4, which plots the ohmic resistance as a function of current density for the Pd containing anode and the ceria-only anode. The ohmic resistance of the cell with only ceria increased from 0.36 to 0.55 Ω cm^2 upon the application of 200 mA/cm^2 and reverted back to its initial value when the cell returned to open circuit. Because ceria must be partially reduced to be conductive, the increased ohmic resistance is likely due to an increase in the average oxidation state of ceria upon application of current. The addition of 1 wt % Pd is too small to provide electronic conductivity directly; however, Pd could affect the average oxidation state of the ceria due to the fact that its presence is expected to dramatically increase the rate of ceria reduction.[26-30] An increased rate of reduction could affect the average oxidation state of the ceria at higher current densities if the rate of ceria oxidation by ions coming through the electrolyte is significant compared to the rate of reduction of ceria by the fuel gas. It is also possible that there is a contribution to the increase in ohmic resistance under current loadings due to an increase in the diffusion pathway for oxygen ions, since a less active catalyst would require more surface area to consume the same number of ions.

Hydrocarbon fuels.— A primary goal in our development of alternative anodes is the direct utilization of hydrocarbons. Therefore, we examined the performance of the ceria-based anodes in methane and *n*-butane to determine how the various catalytic metals perform with the different fuels. Previous studies have shown that there is a good correspondence between how cells perform in *n*-butane and how they perform in fuels with higher molecular weights.[31] Methane tends to be different from other hydrocarbon fuels because it is more difficult to break the C–H bonds in this molecule. Because Ni is known to catalyze the formation of filamentous carbon,[4] we excluded the Ni-doped ceria from these tests because it is unlikely to be stable.

Figure 5 shows V-i polarization curves for 12 μm anodes with 40 wt % ceria and either 1 wt % Pd, 5 wt % Cu, or no added metal at 973 K in dry CH_4. In agreement with previous studies, a reasonable power density of 335 mW/cm^2 could be achieved with the Pd-doped ceria cell, while the performance of the other two cells was very poor.[32] The maximum power density of the Cu-containing cell was only 26 mW/cm^2 and that of the ceria-only cell 9 mW/cm^2. Note also that the open-circuit voltages (OCV) for the Cu-ceria and ceria-only cells were below 0.8 V, compared to more than 1.25 V for the Pd containing cell. It seems clear that the performance of the three cells in CH_4 was limited by the ability of the anode catalysts to break the strong C–H bonds. Cu-ceria and ceria are not effective catalysts for methane oxidation, while Pd-ceria is one of the best catalysts for this reaction.[14]

The same three cells were tested in pure *n*-butane at 973 K, with results shown in Fig. 6. The performance of the ceria-only cell increased dramatically relative to its performance in dry CH_4, exhibiting a maximum power density of 60 mW/cm^2. This almost certainly reflects the relative ease with which the C–H bonds of *n*-butane can be broken, as significant rates for butane oxidation occur at much lower temperatures than rates for CH_4 oxidation on ceria.[33] As in the case with H_2 and CH_4, the addition of Cu again led to a significant improvement in the performance, showing that Cu

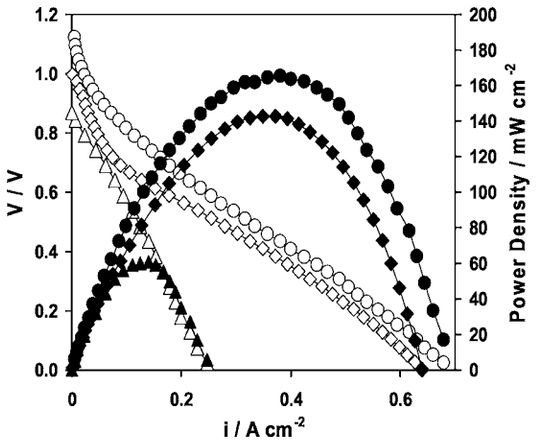

Figure 6. V-i polarization curves for 12 μm CeO_2–M–YSZ anodes with 40 wt % CeO_2 in dry *n*-butane at 973 K. Data is shown for the following metal (M) dopants: circles, 1 wt % Pd, diamonds, 5 wt % Cu, and triangles, no metal.

provides catalytic activity for this reaction. Even more interesting is the fact that the V-i polarization curve for the Cu-ceria cell is similar to what has been reported previously for thicker Cu-ceria anodes.[34] There is pronounced curvature near open circuit that may indicate the need for activation of the reaction by field gradients, such as are described by the Butler-Volmer equation. The maximum power density, 140 mW/cm^2, is also similar to what has been reported for Cu-ceria cells with similar electrolyte thickness.[35]

While the performance of the Cu-ceria and ceria-only cells improved in *n*-butane compared to their performance in CH_4, the same was not true for the Pd-ceria cell. The Pd-ceria cell was only modestly better than the Cu-ceria cell and the maximum power density in *n*-butane, 165 mW/cm^2, was much lower than this same cell achieved in dry CH_4. Furthermore, the V-i curve showed significant curvature near open-circuit, comparable to what is observed on the Cu-ceria cell. Similar observations in a previous study led to the proposal that the Pd surface may be saturated with carbon in the presence of *n*-butane, so that Pd does not enhance the catalytic activity to the same extent as with H_2 or CH_4.[32]

Activation by hydrocarbon deposits.— With dry *n*-butane, it has been shown that gas-phase pyrolysis leads to deposition of polyaromatic tars on the surfaces of the anode at temperatures above approximately 950 K.[4,36] Because these tars are electronically conductive, earlier studies reported that it was possible to prepare high-performance anodes that use carbon for anode conduction.[37] For the present investigation, the use of tar deposits for providing conductivity allowed us to study whether using thin functional layers could limit performance by decreasing the region in which the three-phase boundary (TPB) exists. Therefore, we compared the performance for two cells with functional layer thicknesses of 12 and 50 μm, with tar deposits providing conductivity, to determine whether the electrochemically active region of the anode extends more than 10 μm from the electrolyte interface. We studied ceria-only anodes for this test, as these should be influenced most by catalytic considerations. With low activity for surface reactions, oxygen ions should be able to migrate further into the anode before undergoing reaction at the surface.

The ohmic resistance and maximum power densities of ceria-only cells with 12 and 50 μm thick anodes at 973 K in dry *n*-butane, after exposure to *n*-butane for 4 h, were 0.29 and 0.35 Ω cm^2, as shown in Table III. This difference in the ohmic resistances is significantly lower than the difference reported in Table I, showing that the carbon deposits are contributing to the conductivity of the functional layer. However, even with the higher ohmic resistance, the cell with the 50 μm functional layer showed a higher power density, 75 mW/cm^2 compared to 60 mW/cm^2 on the 12 μm anode. This higher power density with the thicker functional layer implies that making the functional layer too thin limits performance. The observation that the nonohmic contribution to the electrode impedances of Pd-doped anodes operating on H_2 were not affected by functional layer thickness (Fig. 1b) shows that the electrochemically active region of the anode extends farther into the anode when the catalytic activity is low.

Table III. Ohmic resistance and performance of CeO_2–YSZ anodes with 40 wt % CeO_2 at 973 K in *n*-butane for various anode thicknesses.

Thickness	$R_{\Omega\ \text{total}}$ (Ω cm^2)	Power density (mW cm^{-2})
10 μm	0.29	61
50 μm	0.35	77
100 μm	0.82	58

Discussion

The use of functional layers for both SOFC anodes and cathodes is certainly not new.[38,39] However, in most cases, the same materials are used in the functional and conduction layers, with only the structure of the two layers being changed. The use of an entirely different set of materials in these two layers, with properties optimized for the role that each layer plays, is less common. The present results further demonstrate the promise of using this approach, with thin functional layers, for the development of high-performance ceramic anodes.

For the same reasons that composites prepared by impregnation are attractive for conventional electrodes, they are also attractive for preparing functional layers. First, essentially any metal or oxide can be added to enhance catalytic activity, so that there is great compositional flexibility in preparing functional layers by impregnation. Second, different sintering temperatures can be used for the added catalysts and the backbone structure, making it much easier to optimize the microstructure of the electrode. Third, the thermal expansion properties of composites prepared by impregnation are similar to that of the backbone material.[40]

While the use of thin functional layers for the anode is promising, the present results also point toward areas where future work is required to make impregnated electrodes practical. Most important is the need to achieve stable conductivity within the functional layer. Surprisingly, even with the addition of 60 wt % ceria, there was a loss of conductivity after heating to 1173 K, probably because of ceria sintering. Because 60 wt % ceria corresponds to almost 50 vol % ceria, most of the available porosity was already filled with ceria in these anodes, making it unlikely that impregnating even larger amounts of ceria will provide stable conductivity.

To achieve improved conductivity in functional layers prepared by impregnation, it will be necessary either to replace ceria with a substance having better electronic conductivity or to add electronic conductivity to the porous backbone. Because the catalytic properties of ceria are so crucial, it will be difficult to replace ceria with a better electronic conductor without losing the catalytic activity. Ceria appears to be unique in its ability to enhance the oxidation activity of metal catalysts.[14] Therefore, we suggest that adding electronic conductivity to the backbone is the most promising approach, rather than trying to replace ceria. It is important to remember that the conductivity of the functional layer does not need to be significantly greater than 0.02 to 0.05 S/cm, so long as this layer is kept thin. Because it seems optimal to have the porous backbone be based on zirconia for maintaining good connectivity with the electrolyte, we suggest that one promising approach for establishing conductivity is through the use of dopants, such as Ti or Nb.[41,42] An alternative would be to make the backbone itself a composite, such as by using a mixture of YSZ and doped $SrTiO_3$.[43]

Because oxide catalysts tend to have much lower activity than metals for oxidation reactions, the addition of dopant-levels of metal catalysts is probably essential for achieving high performance. The amount of metal required for catalysis is small, so that this should not affect the stability of the electrode towards oxidation and reduction cycles. Interestingly, the results in this study show the optimal choice of catalyst depends on the fuel that is being used. Ni-doped anodes performed well for operation in H_2 and could be used for operation on sulfur-free syngas. For direct utilization of hydrocarbons, Cu appears to be as effective as Pd.

As with any supported metal catalyst, it is important to maintain the metal in a highly dispersed state to maximize the surface area for reaction. While this can be difficult at high temperatures, there has been progress in developing supported metal catalysts with high thermal stability. Fornasiero and coworkers have prepared ceria-encapsulated metals that appear to show excellent thermal stability.[44]

Finally, there appears to be an optimal thickness for the anode functional layer that will likely depend on the catalytic activity of the material used. The low anode impedance observed with Pd-ceria anodes in humidified H_2 suggest that 10 μm is sufficient in this case but thicker functional layers may be required for less reactive fuels and less active electrodes.

Conclusions

Anode functional layers, prepared by impregnation of ceria and catalytic metals, can provide excellent anode performance. While anodes with precious-metal catalysts may exhibit the best all-around performance, low anode overpotentials can also be achieved using base metals, such as Ni when the fuel is H_2. Cu can be almost as effective as Pd for direct utilization of *n*-butane. While freshly prepared impregnated ceria provides sufficient conductivity for thin functional layers, high-temperature sintering leads to a loss in conductivity, so that improvements in the conductivity are still required.

Acknowledgments

This work was funded by the U.S. Department of Energy's Hydrogen Fuel Initiative.

The University of Pennsylvania assisted in meeting the publication costs of this article.

References

1. N. Q. Minh, *J. Am. Ceram. Soc.*, **76**, 563 (1993).
2. A. Atkinson, S. Barnett, R. J. Gorte, J. T. S. Irvine, A. J. McEvoy, M. B. Mogensen, S. Singhal, and J. Vohs, *Nat. Mater.*, **3**, 17 (2004).
3. Y. Matsuzaki and I. Yasuda, *Solid State Ionics*, **132**, 261 (2000).
4. S. McIntosh and R. J. Gorte, *Chem. Rev. (Washington, D.C.)*, **104**, 4845 (2004).
5. G. Rietveld, P. Nammensma, and J. P. Ouweltjes, in *Solid Oxide Fuel Cells VII*, H. Yokokawa and S. C. Singhal, Editors, PV 2001-16, p. 125, The Electrochemical Society Proceedings Series, Pennington, NJ (2001).
6. S. Tao and J. T. S. Irvine, *Chem. Rec.*, **4**, 83 (2004).
7. J. Liu, B. D. Madsen, A. Ji, and S. A. Barnett, *Electrochem. Solid-State Lett.*, **5**, A122 (2002).
8. O. A. Marina, N. L. Canfield, and J. W. Stevenson, *Solid State Ionics*, **149**, 21 (2002).
9. J. Sfeir, P. A. Buffat, P. Mockli, N. Xanthopoulos, R. Vasquez, H. J. Mathieu, J. Van Herle, and K. R. Thampi, *J. Catal.*, **202**, 229 (2001).
10. Y. H. Huang, R. I. Dass, Z. L. Xing, and J. B. Goodenough, *Science*, **312**, 254 (2006).
11. Y. H. Huang, R. I. Dass, J. C. Denyszyn, and J. B. Goodenough, *J. Electrochem. Soc.*, **153**, A1266 (2006).
12. R. Mukundan, E. L. Brosha, and F. H. Garzon, *Electrochem. Solid-State Lett.*, **7**, A5 (2004).
13. M. D. Gross, J. M. Vohs, and R. J. Gorte, *Electrochem. Solid-State Lett.*, **10**, B65 (2007).
14. A. Trovarelli, *Catal. Rev. - Sci. Eng.*, **38**, 439 (1996).
15. S. Park, R. J. Gorte, and J. M. Vohs, *J. Electrochem. Soc.*, **148**, A443 (2001).
16. Y. Huang, J. M. Vohs, and R. J. Gorte, *J. Electrochem. Soc.*, **151**, A646 (2004).
17. Y. Jiang, A. V. Virkar, and F. Zhao, *J. Electrochem. Soc.*, **148**, A1091 (2001).
18. K. Sasaki and J. Maier, *Solid State Ionics*, **134**, 303 (2000).
19. S. Jung, C. Lu, H. He, K. Ahn, R. J. Gorte, and J. M. Vohs, *J. Power Sources*, **154**, 42 (2006).
20. O. Costa-Nunes, R. J. Gorte, and J. M. Vohs, *J. Mater. Chem.*, **15**, 1520 (2005).
21. T. Kim, K. Ahn, J. M. Vohs, and R. J. Gorte, *J. Power Sources*, **164**, 42 (2007).
22. X. Qi and M. Flytzani-Stephanopoulos, *Ind. Eng. Chem. Res.*, **43**, 3055 (2004).
23. H. Oguchi, T. Nishiguchi, T. Matsumoto, H. Kanai, K. Utani, Y. Matsumura, and S. Imamura, *Appl. Catal., A*, **281**, 69 (2005).
24. Y. Liu, T. Hayakawa, K. Suzuki, S. Hamakawa, T. Tsunoda, T. Ishii, and M. Kumagai, *Appl. Catal., A*, **223**, 137 (2002).
25. C. Lu, W. L. Worrell, J. M. Vohs, and R. J. Gorte, *J. Electrochem. Soc.*, **150**, A1357 (2003).
26. M. Shelef, G. W. Graham, and R. W. McCabe, in *Catalysis by Ceria and Related Materials*, A. Trovarelli, Editor, p. 343, Imperial College Press, London (2002).
27. G. S. Zafiris and R. J. Gorte, *J. Catal.*, **139**, 561 (1993).
28. H. Cordatos and R. J. Gorte, *J. Catal.*, **159**, 112 (1996).
29. M. Y. Smirnov and G. W. Graham, *Catal. Lett.*, **72**, 39 (2001).
30. J. Kaspar, P. Fornasiero, and N. Hickey, *Catal. Today*, **77**, 419 (2003).
31. H. Kim, S. Park, J. M. Vohs, and R. J. Gorte, *J. Electrochem. Soc.*, **148**, A693 (2001).
32. S. McIntosh, J. M. Vohs, and R. J. Gorte, *Electrochem. Solid-State Lett.*, **6**, A240 (2003).
33. S. Zhao and R. J. Gorte, *Appl. Catal., A*, **277**, 129 (2004).
34. S. McIntosh, J. M. Vohs, and R. J. Gorte, *J. Electrochem. Soc.*, **150**, A1305 (2003).
35. R. J. Gorte, S. Park, J. M. Vohs, and C. Wang, *Adv. Mater. (Weinheim, Ger.)*, **19**, 1465 (2000).
36. T. Kim, G. Liu, M. Boaro, S.-I. Lee, J. M. Vohs, R. J. Gorte, O. H. Al-Madhi, and B. O. Dabbousi, *J. Power Sources*, **155**, 231 (2006).
37. S. McIntosh, J. M. Vohs, and R. J. Gorte, *J. Electrochem. Soc.*, **150**, A470 (2003).
38. F. Zhao and A. V. Virkar, *J. Power Sources*, **141**, 79 (2005).
39. V. Vashook, J. Zosel, R. Muller, P. Shuk, L. Vasylechko, H. Ullmann, and U. Guth, *Fuel Cells*, **6**, 293 (2006).
40. Y. Huang, K. Ahn, J. M. Vohs, and R. J. Gorte, *J. Electrochem. Soc.*, **151**, A1592 (2004).
41. K. E. Swider and W. L. Worrell, *J. Electrochem. Soc.*, **143**, 3706 (1996).
42. J. T. S. Irvine, D. P. Fagg, J. Labrincha, and F. M. B. Marques, *Catal. Today*, **38**, 467 (1997).
43. H. He, Y. Huang, J. M. Vohs, and R. J. Gorte, *Solid State Ionics*, **175**, 171 (2004).
44. T. Montini, L. De Rogatis, V. Gombac, P. Fornasiero, and M. Graziani, *Appl. Catal., B*, **71**, 125 (2006).